Available online at www.sciencedirect.com
ScienceDirect
Trans. Nonferrous Met. Soc. China 21(2011) 1767−1772
Transactions of Nonferrous Metals Society of China
www.tnmsc.cn

Hydrothermal synthesis of monodisperse $Zn_xCd_{1-x}S$ spheres and their photocatalytic properties

JIA Zhi-fang, WANG Fu-min, XIN Feng

School of Chemical Engineering and Technology, Tianjin University, Tianjin 300072, China

Received 19 August 2010; accepted 14 January 2011

Abstract: Monodisperse $Zn_xCd_{1-x}S$ spheres were successfully fabricated with a high yield by a facile hydrothermal route. The as-prepared samples were characterized by X-ray diffractometry, scanning electron microscopy and UV-vis diffusion reflectance spectroscopy. The results indicate that all the prepared samples have the same hexagonal wurtzite phase and exhibit good size uniformity and regularity. Degradation of rhodamine-B (RhB) was used to evaluate the photocatalytic activities of $Zn_xCd_{1-x}S$ samples. $Zn_{0.4}Cd_{0.6}S$ possessed the best photocatalytic activity and exhibited high stability during the reaction.

Key words: monodisperse $Zn_xCd_{1-x}S$ spheres; hydrothermal synthesis; solid solution; photocatalytic activity

1 Introduction

Semiconductor-based photocatalysis offers an advanced technology for the decomposition of the soluble dyes in wastewater and various researches have been focused on exploiting novel and more efficient photocatalysts [1−5]. One of the most well-known semiconductor photocatalyst, CdS, is an interesting visible-light-sensitive photocatalyst material owing to its narrow band gap (2.4 eV). However, the photocatalytic properties of CdS are limited due to its photocorrosion in photocatalytic reactions. On the other hand, ZnS is another metal sulfide that has been used as photocatalyst. The band gap of ZnS is 3.66 eV, which is too large for visible light response. $Zn_xCd_{1-x}S$ nanocrystals used as the solid solutions of CdS and ZnS have been widely used in optoelectronic devices [6−7]. In addition, $Zn_xCd_{1-x}S$ nanoparticles can produce hydrogen from water splitting under visible light irradiation with higher efficiency than pure ZnS and CdS nanoparticles [8−9], but they have seldom been used to degrade organic dyes [10]. Recently, hydrothermal synthesis has been reported as a good strategy to prepare $Zn_xCd_{1-x}S$ nanoparticles [11−12]. However, in the hydrothermal process of synthesizing $Zn_xCd_{1-x}S$ nanoparticles, some severe conditions are required, such as high temperature (180−240 °C) and long reaction time (24 h). It is highly desirable to synthesize $Zn_xCd_{1-x}S$ under mild conditions.

Herein, a facile one-step hydrothermal method was presented to fabricate monodisperse $Zn_xCd_{1-x}S$ spheres at relatively low temperature of 140 °C without the use of surfactant. Moreover, the photocatalytic activities of the samples were evaluated by the degradation of RhB under tungsten halogen lamp irradiation.

2 Experimental

2.1 Synthesis of samples

All the reagents used in the experiments were analytical grade and used without further purification. In a typical synthesis, zinc acetate and cadmium acetate in appropriate molar ratios and with a total molar amount of 3 mmol were dissolved in 40 mL deionized water, thiourea (40 mmol) was added with continuous stirring, and then the mixture was transferred into a Teflon-lined stainless steel autoclave with a capacity of 60 mL. Finally, the autoclave was sealed and maintained at 140 °C for 5 h and then cooled to room temperature naturally. The precipitate was collected by centrifugation, and washed several times with deionized water and ethanol, and then dried in an oven at 80 °C for 5 h.

Foundation item: Project (20776016) supported by the National Natural Science Foundation of China; Project (20876109) supported by Program for New Century Excellent Talents in University of China
Corresponding author: WANG Fu-min; Tel: +86-22-27890041; Fax: +86-22-27890041; E-mail: wangfumin@tju.edu.cn
DOI: 10.1016/S1003-6326(11)60928-X

2.2 Characterization

The X-ray diffraction (XRD) patterns were recorded on a Rigaku D/max 2500 diffractometer with Cu-K_α radiation at a scanning speed of 8 (°)/min from 20 to 60°. The scanning electron microscopy (SEM) characterizations were performed on a Nanosem 430 field emission scanning electron microscope. The UV-vis absorption spectra were measured on a Shimadzu UV−2550 spectrophotometer using $BaSO_4$ as a reference in wavelength of 200–800 nm.

2.3 Evaluation of photocatalytic activity

The photocatalytic activities of the monodisperse $Zn_xCd_{1-x}S$ spheres were evaluated by degradation of rhodamine B (RhB) under a 300 W tungsten halogen lamp (Philips Q/YXKC33). An amount of 0.05 g photocatalyst was suspended in a 100 mL aqueous solution with 5 mg/L RhB. The distance betweens light source and the top of the solution was about 25 cm. Before illumination, the suspensions were magnetically stirred in dark for 30 min to ensure the establishment of an adsorption-desorption equilibrium between the photocatalysts and RhB. At given time intervals, 3 mL reaction solution was sampled and centrifuged to remove photocatalyst powders. Then, the UV-vis adsorption spectrum of the centrifugated solution was recorded using an UV-vis spectrophotometer. The stability and resuability of the photocatalyst were examined by repetitive use of the catalyst under the same conditions.

3 Results and discussion

3.1 Crystalline phase and morphology

The crystallinity and phase purity of the products were characterized by XRD analysis. Figure 1 shows the XRD patterns of the as-prepared products with different molar ratios of Zn to Cd. No characteristic peaks of other impurities are observed, and all the samples have the same hexagonal wurtzite phase. However, the intensity of diffraction peaks increases with decreasing x values, indicating the formation of a highly crystalline product with the increase of Cd content. The diffraction peaks shift to a higher-angle side as the x value increases. The successive shift of the XRD pattern indicates that the crystal obtained is not a mixture of ZnS and CdS phases but $Zn_xCd_{1-x}S$ solid solutions [13]. The radius of Zn^{2+} (0.74 Å) is smaller than that of Cd^{2+} (0.97 Å), so it is considered that Zn^{2+} incorporates in CdS lattice or enters its interstitial sites [14].

The size and morphology of the products synthesized with different x values were observed by SEM. Figure 2 presents the typical SEM images of $Zn_xCd_{1-x}S$ samples. It can be seen that all the products are composed of a large quantity of monodisperse $Zn_xCd_{1-x}S$ spheres with diameter of 150−250 nm. An interesting feature is that each sphere is constructed by many smaller particles with size of 20−30 nm. The spheres are loose and very rough. While x value decreases to 0.2, the spheres become more tight and smooth. It is fascinating to note that $Zn_xCd_{1-x}S$ nanoparticles can self-aggregate into sphere-like structure in the absence of surfactants or organic additives.

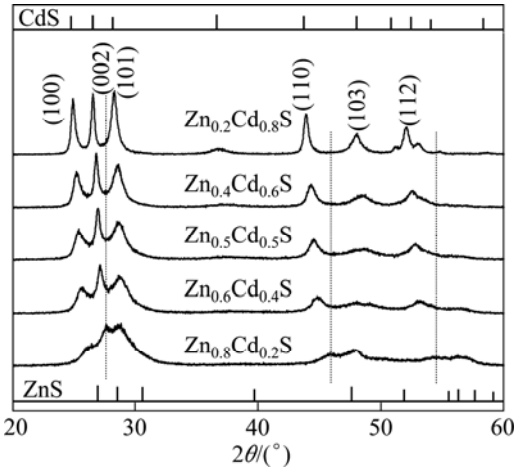

Fig. 1 XRD patterns of $Zn_xCd_{1-x}S$ samples prepared by hydrothermal method

3.2 UV–vis diffuse reflectance spectrum

The optical absorption of the $Zn_xCd_{1-x}S$ samples was measured using an UV-vis spectrometer. Figure 3 shows the UV-vis diffusion reflectance absorption spectra of the $Zn_xCd_{1-x}S$ samples. It could be seen that the $Zn_xCd_{1-x}S$ products have intense absorption bands with steep edges in the visible-light region. The steep shape of the spectra also indicates that the visible light absorption of $Zn_xCd_{1-x}S$ is ascribed to the transition from the valence band to the conduction band but not to the transition from the impurity levels to the conduction band [15−16]. The absorption edges of the $Zn_xCd_{1-x}S$ solid solutions are gradually red shifted as the amount of Cd increases. Correspondingly, the band gaps of the samples are estimated to be 2.14−3.25 eV from the onsets of the absorption edges.

3.3 Photocatalytic activity

The photocatalytic activities of the $Zn_xCd_{1-x}S$ samples were evaluated by the degradation of tetraethylated rhodamine B under 300 W tungsten halogen lamp irradiation. The characteristic absorption at about 553 nm corresponding to RhB was used to monitor

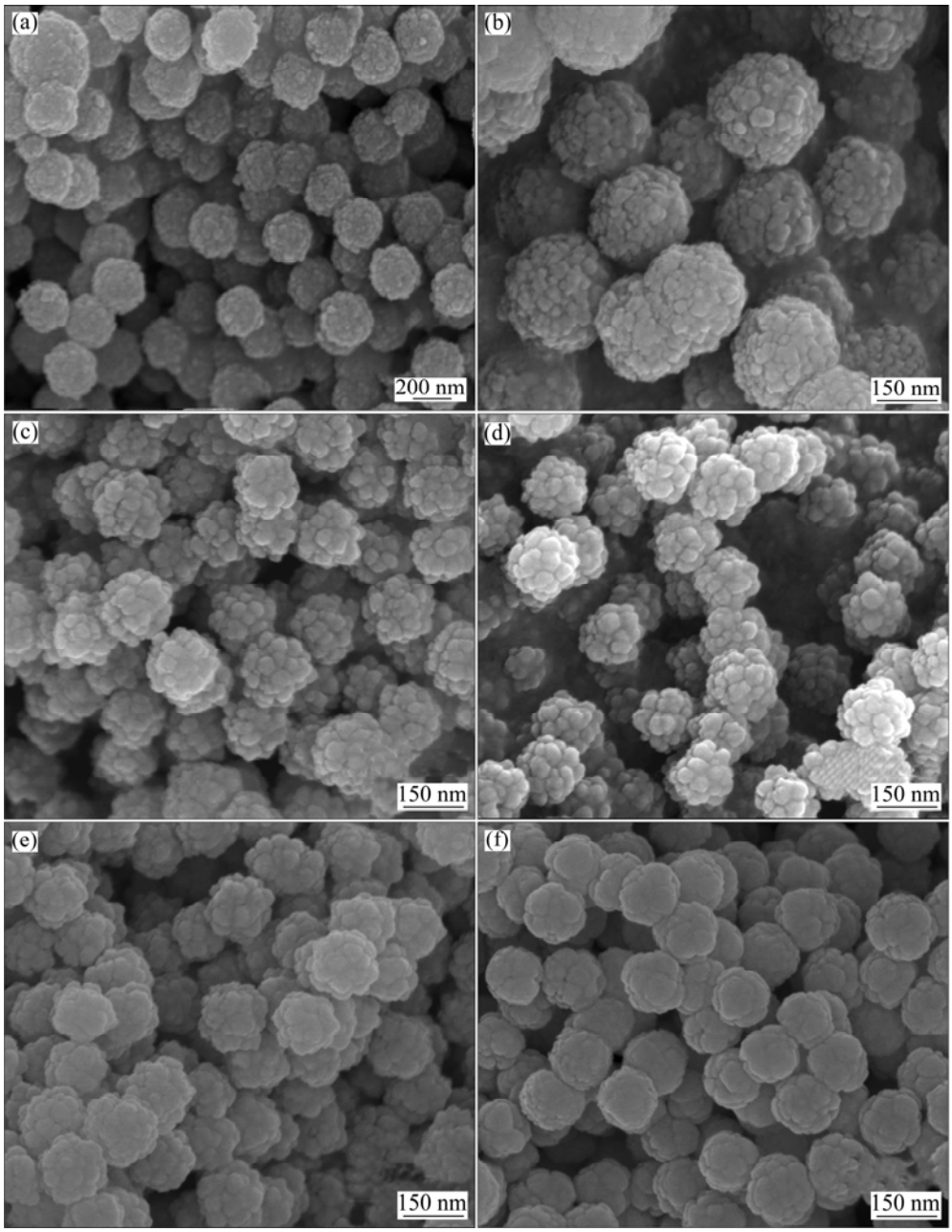

Fig. 2 SEM images of $Zn_xCd_{1-x}S$ samples: (a) x=1.0; (b) x=0.8; (c) x=0.6; (d) x=0.5; (e) x=0.4; (f) x=0.2

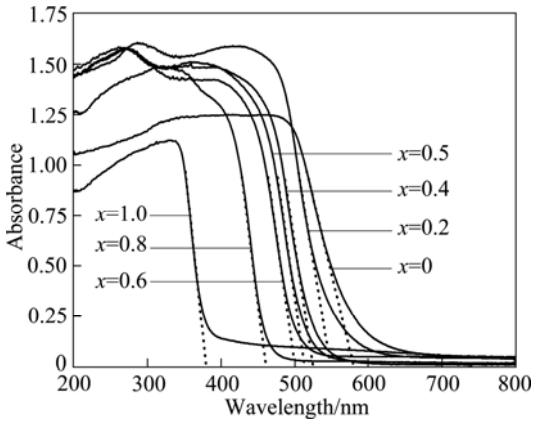

Fig. 3 UV-vis diffusion reflectance spectra of as-synthesized $Zn_xCd_{1-x}S$ samples

the concentration of RhB, C was the absorption of RhB at the wavelength of 553 nm and C_0 was the absorption of RhB after the adsorption equilibrium on $Zn_xCd_{1-x}S$ photocatalysts before irradiation. As a comparison, photodegradation of RhB over P25 was also performed. Figure 4 displays the degradation process of RhB with hydrothermally synthesized $Zn_xCd_{1-x}S$ samples as photocatalysts. It can be clearly observed that RhB has underwent a significant degradation and most of the samples exhibit higher photoactivity than P25. Among them, $Zn_{0.4}Cd_{0.6}S$ shows the highest photocatalytic activity, the photodegradation efficiency reaches 98.7% after a reaction of 180 min.

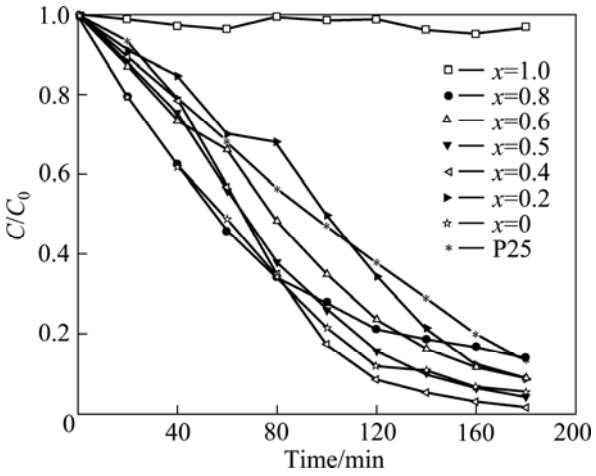

Fig. 4 Photodegradation of RhB dye with $Zn_xCd_{1-x}S$ as photocatalyst vs irradiation time

The main reason for different activities of $Zn_xCd_{1-x}S$ samples should be attributed to the difference of band gap. The conduction band of $Zn_xCd_{1-x}S$ consists of hybridized Zn 4s4p with Cd 5s5p [17] and the position of conduction band becomes more negative with the increase of Cd, thus, the band gap of $Zn_xCd_{1-x}S$ can be adjusted by changing the molar ratio of Zn to Cd. What is more, XING et al [18] also proposed that an appropriate amount of doping-Zn into the lattice or interstitial of CdS provided suitable impurity energy levels which made the excited electrons from the valence band of CdS easily inject into the conduction band. The highest photocatalytic activity of $Zn_{0.4}Cd_{0.6}S$ may be due to its optimum band gap and a moderate position of conduction band. Compared to other $Zn_xCd_{1-x}S$ samples, it is easier to make the excited electrons from the valence band inject into the conduction band for $Zn_{0.4}Cd_{0.6}S$.

Figure 5 displays the temporal evolution of the spectra during the photodegradation process of RhB mediated by $Zn_{0.4}Cd_{0.6}S$. RhB has strong absorption at 553 nm. Blank test demonstrates that the degradation of RhB is rather low. When the photocatalytic experiments were carried out under tungsten halogen lamp irradiation, as the exposure time extended, the absorption intensity decreased gradually and the absorption peak blue-shifted. After 180 min, the absorption peak almost completely disappeared and the initial pink color of RhB solution faded. This result agrees well with the report by WU et al [19]. According to their report, the blue-shift of the absorption band is caused by de-ethylation of RhB because of the attack by one of the active oxygen species on the N-ethyl group. When the de-ethylated process is fully completed, the absorption band shifts to 498 nm and RhB is turned to rhodamine. Rhodamine is then

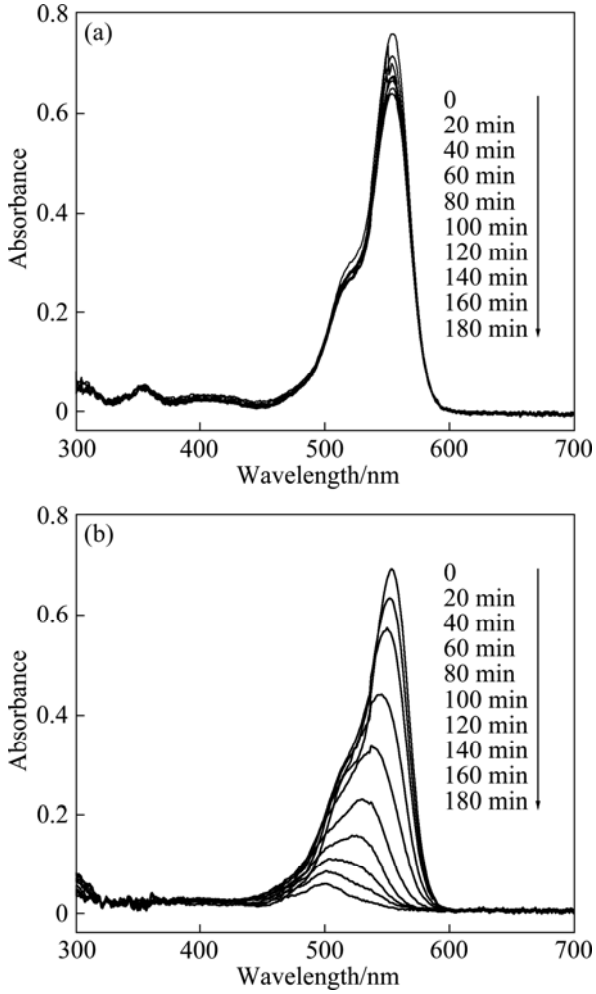

Fig. 5 Absorbance spectra changes of RhB solution in the presence of $Zn_{0.4}Cd_{0.6}S$: (a) Blank test in dark; (b) Under tungsten halogen lamp irradiation

gradually decomposed due to the further destruction of the conjugated structure. The sharp decrease and shift of the absorption peak indicate the good photocatalytic activity of the as-synthesized $Zn_{0.4}Cd_{0.6}S$.

From the view of application, the stability of a photocatalyst is important and necessary. In our experiments, $Zn_{0.4}Cd_{0.6}S$ was used as a representative photocatalyst to evaluate the stability. As shown in Fig. 6, the photocatalytic activity did not exhibit obvious loss after three recycles for the photodegradation of RhB, which indicates that the $Zn_{0.4}Cd_{0.6}S$ has high stability and does not suffer from photocorrosion during the photodegradation of RhB. $Zn_{0.4}Cd_{0.6}S$ shows a good potential in practical application.

4 Conclusions

1) A series of monodisperse $Zn_xCd_{1-x}S$ spheres are successfully synthesized with a high yield by a simple

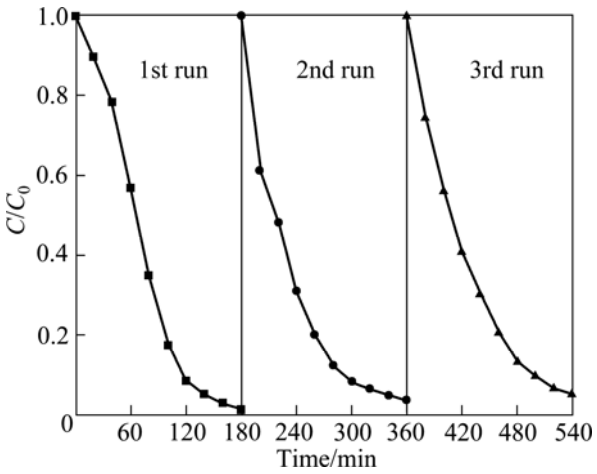

Fig. 6 Photocatalytic degradation of RhB in the presence of $Zn_{0.4}Cd_{0.6}S$

hydrothermal method.

2) The absorption properties can be tuned through changing the compositions, meanwhile, the composition of $Zn_xCd_{1-x}S$ also has a great impact on the photocatalytic activity.

3) Among all the prepared samples, $Zn_{0.4}Cd_{0.6}S$ exhibits the best photocatalytic activity to the degradation of RhB. After three recycles for the photodegradation of RhB, $Zn_{0.4}Cd_{0.6}S$ does not exhibit obvious significant loss in activity, which indicates its considerable stability of the catalyst. This suggests that $Zn_{0.4}Cd_{0.6}S$ has potential future applications in environmental purification.

References

[1] FANG Hai-bo, XU Ming-xia, GE Lei, HE Zhi-yuan. Synthesis and photocatalytic properties of $InVO_4$ sol containing nanocrystals by mild hydrothermal processing [J]. The Chinese Journal of Nonferrous Metals, 2006, 16(s): 373−376. (in Chinese)

[2] FAN Cai-mei, XUE Peng, SUN Yan-ping. Preparation of nano-TiO_2 doped with cerium and its photocatalytic activity[J]. Journal of Rare Earths, 2006, 24(3): 309−313. (in Chinese)

[3] SONG Li-min, ZHANG Shu-juan, CHEN Bin, SUN Dong-lan. Highly active NiO-CaO photocatalyst for degrading organic contaminants under visible-light irradiation [J]. Catal Commun, 2009, 10(5): 421−423.

[4] DONG Lin, CAO Guo-xi, MA Ying, JIA Xiao-lin, YE Guo-tian, GUAN Shao-kang. Enhanced photocatalytic degradation properties of nitrogen-doped titania nanotube arrays [J]. The Chinese Journal of Nonferrous Metals, 2009, 19(6): 1583−1587. (in Chinese)

[5] YAO Mao-hai, TANG You-gen, ZHANG Li, YANG Hai-hua, YAN Jian-hui. Photocatalytic activity of CuO towards HER in catalyst from oxalic acid solution under simulated sunlight irradiation[J]. The Chinese Journal of Nonferrous Metals, 2010, 20(10): 1944−1949. (in Chinese)

[6] ZHONG Xin-hua, FENG Yao-yu, KNOLL W, HAN Ming-yong. Alloyed $Zn_xCd_{1-x}S$ nanocrystals with highly narrow luminescence spectral width[J]. J Amer Chem Soc, 2003, 125(44): 13559−13563.

[7] WANG Wen-zhong, GERMANENKO I, EL-SHALL M S. Room-temperature synthesis and characterization of nanocrystalline CdS, ZnS, and $Zn_xCd_{1-x}S$ [J]. Chem Mater, 2002, 14(7): 3028−3033.

[8] WANG Lu, WANG Wen-zhong, SHANG Meng, YIN Wen-zong, SUN Song-mei, ZHANG Ling. Enhanced photocatalytic hydrogen evolution under visible light over $Cd_{1-x}Zn_xS$ solid solution with cubic zinc blend phase [J]. International Journal of Hydrogen Energy, 2010, 35(1): 19−25.

[9] ZHANG Kai, JING Deng-wei, XING Chan-juan, GUO Lie-jin. Significantly improved photocatalytic hydrogen production activity over $Cd_{1-x}Zn_xS$ photocatalysts prepared by a novel thermal sulfuration method [J]. International Journal of Hydrogen Energy, 2007, 32(18): 4685−4691.

[10] SONG Li-min, ZHANG Shu-juan, CHEN Bin, GE Jing-jie, JIA Xi-cheng. Fabrication of ternary zinc cadmium sulfide photocatalysts with highly visible-light photocatalytic activity [J]. Catal Commun, 2010, 11(5): 387−390.

[11] SHI Jian-ying, YAN Hong-jian, WANG Xiu-li, LEI Zhi-bin, LI Can. Composition-dependent optical properties of $Zn_xCd_{1-x}S$ synthesized by precipitable-hydrothermal process [J]. Solid State Communications, 2008, 146(5−6): 249−252.

[12] ZU Sheng-nan, WANG Zhi-yu, LIU Bo, FAN Xian-ping, QIAN Guo-dong. Synthesis of nano-$Cd_xZn_{1-x}S$ by precipitate-hydrothermal method and its photocatalytic activities [J]. Journal of Alloys and Compounds, 2009, 476(1−2): 689−692.

[13] TSUJI I, KATO H, KOBAYASHI H, KUDO A. Photocatalytic H_2 evolution reaction from aqueous solutions over band structure controlled $(AgIn)_xZn_{2(1-x)}S_2$ solid solution photocatalysts with visible-light response and their surface nanostructures[J]. J Amer Chem Soc, 2004, 126(41): 13406−13413.

[14] NIEN Y T, CHEN P W, CHEN I G. Synthesis and characterization of $Zn_xCd_{1-x}S$: Cu, Cl red electroluminescent phosphor powders [J]. J Alloys Compd, 2008, 462 (1−2): 398−403.

[15] KUDO A, SEKIZAWA M. Photocatalytic H_2 evolution under visible light irradiation on Ni-doped ZnS photocatalyst [J]. Chem Commun, 2000, 1371−1372.

[16] KUDO A, SEKIZAWA M. Photocatalytic H_2 evolution under visible light irradiation on $Zn_{1-x}Cu_xS$ solid solution [J]. Catal Lett, 1999, 58(4): 241−243.

[17] LIU Guan-jie, ZHAO Liang, MA Li-jing, GUO Lie-jin. Photocatalytic H_2 evolution under visible light irradiation on a novel $Cd_xCu_yZn_{1-x-y}S$ catalyst [J]. Catal Commun, 2008, 9(1): 126−130.

[18] XING Chan-juan, ZHANG Yao-jun, YAN Wei, GUO Lie-jin. Band structure-controlled solid solution of $Cd_{1-x}Zn_xS$ photocatalyst for hydrogen production by water splitting [J]. Int J Hydrogen Energy, 2006, 31(14): 2018−2024.

[19] WU Tai-xing, LIU Guang-ming, ZHAO Jin-cai, HIDAKA H, SERPONE N. Photoassisted degradation of dye pollutants V self-photosensitized oxidative transformation of rhodamine B under visible light irradiation in aqueous TiO_2 dispersions[J]. J Phys Chem B, 1998, 102(30): 5845−5851.

水热合成单分散球状 $Zn_xCd_{1-x}S$ 及其光催化性质

贾志方，王富民，辛 峰

天津大学 化工学院，天津 300072

摘 要：采用简单的水热合成路线制备高产量单分散球状 $Zn_xCd_{1-x}S$，通过 X 射线衍射、扫描电镜以及紫外−可见漫反射对所得的产物进行表征。结果表明，所得产物呈现六方相纤锌矿结构，并且 $Zn_xCd_{1-x}S$ 产物呈现出很好的均匀性与规则性。采用光催化降解罗丹明 B 反应来评价 $Zn_xCd_{1-x}S$ 的光催化活性。其中，$Zn_{0.4}Cd_{0.6}S$ 具有最高的催化活性，并且在降解反应过程中表现出很高的稳定性。

关键词：单分散球状 $Zn_xCd_{1-x}S$；水热合成；固溶体；光催化活性

(Edited by FANG Jing-hua)